Excellent field emitters: onion-shaped tipped carbon nanotubes

ARTICLE *in* THE JOURNAL OF PHYSICAL CHEMISTRY C · MARCH 2010

Impact Factor: 4.77

4 AUTHORS, INCLUDING:

Rujia Zou

Donghua University

96 PUBLICATIONS **76** CITATIONS

SEE PROFILE

Zhigang Chen

Beijing University of Civil Engineering and …

220 PUBLICATIONS **4,263** CITATIONS

SEE PROFILE

Excellent Field Emitters: Onion-Shaped Tipped Carbon Nanotubes

Junqing Hu,* Rujia Zou, Yangang Sun, and Zhigang Chen

State Key Laboratory for Modification of Chemical Fibers and Polymer Materials, College of Materials Science and Engineering, Donghua University, Shanghai 201620, P. R. China

Received: February 12, 2010; Revised Manuscript Received: March 27, 2010

Large-scale synthesis of highly graphitic carbon nanotubes (with a diameter of ∼5−8 nm) from a thermal reaction of activated carbon and Bi_2O_3 powders, which was grown *via* a carbon-thermal reduction and Bi catalyzed vapor−liquid−solid process has been obtained. Individual carbon nanotubes were terminated with an onion-shaped carbon tip, which has never been observed in growth of a carbon nanotube. Field emitters made from the present carbon nanotubes exhibit excellent emission properties: they can be operated at a very large current density of ∼145 mA/cm^2 at a low voltage of 5.5 V/μm, and possess a long period (>32 h) of high emission stability at a high emission current density of ∼9 mA/cm^2 and under a constant applied voltage. These properties are equally important for high image quality in field emission display fabrication. Hence, as-fabricated CNTs could act as excellent electron emitters and have great potential application in field emission panel displays.

Introduction

Since the identification of carbon nanotubes (CNTs),[1] extensive efforts have been made to prepare well-graphitized (single-, double-, and multiwalled) CNTs, analyze their unique properties, and find potential applications.[2–4] The prevalent synthesis methods include arc-discharge,[5] laser ablation,[6] and chemical vapor deposition (CVD) (including catalytic pyrolysis of hydrocarbons).[2,7] The yield, structure, and properties of CNTs are strongly dependent on the preparation and reaction conditions of these methods. Also, these methods often require complex preparation and toxic gaseous precursors.[5–7] In our previous study, we successfully developed a new carbon thermal reaction route by using activated carbon powders as a carbon source for the synthesis of uniform crystalline carbon microtubes (diameter of ∼1−2 μm).[8,9] The method offered simplicity (in both source materials and synthetic process), and high yield, for production of carbon tubular materials. Therefore, we predicted that highly graphitic CNTs may be synthesized via this similar carbon thermal reaction route. Herewith, we report on the experimental verification of our predictions: large-scale synthesis of highly graphitic carbon nanotubes (with a diameter of ∼5−8 nm) from a thermal reaction of activated carbon and Bi_2O_3 powders. To our knowledge, an individual carbon nanotube terminated with a onion-shaped carbon has never been observed in the growth of carbon nanotubes. Keeping in mind that carbon microtubes may also be synthesized using a similar technique,[8,9] we propose that the method is a universal oxide carbon-thermal reaction route toward growth of crystalline graphitic carbon micro/nanotubes.

CNTs have attracted much attention as an electron source because of their high aspect ratio, remarkably high electrical conductivity, high mechanical strength, and high thermal stability.[10–12] They have potential application in cathodes of a flat-panel display, cathode-ray-tube lighting elements, and field-emission source. However, the CNTs of electron field emission display (FED) do not immediately come into reliable commercial products. Two of the technical issues about FED fabrication and application are the lack of high emission current density for FED fabrication and long period emission stability in high current density.[13] Therefore, the search of a new promising cathode material possessing a large and stable field emission current density has recently received considerable attention. In the present study, the field emitters fabricated from as-synthesized carbon nanotubes can work at a very large current density of ∼145 mA/cm^2 at a low voltage of 5.5 V/μm, and possess a long period (>32 h) of emission stability at a high emission current density of ∼9 mA/cm^2 and under a constant applied voltage. The large emission current and long period stability properties are equally important for field emission display fabrication with high image quality. Hence, the excellent field emission properties of the as-synthesized carbon nanotubes make them highly promising for field emitters.

Experimental Section

The carbon nanotubes were synthesized through thermal reactions using a mixture of Bi_2O_3 and activated carbon powders as source materials in a horizontal high-temperature resistance furnace. A quartz tube, into which a thinner quartz tube was inserted as a liner, was set inside a resistance furnace; one long strip-like alumina wafer was used as the substrate and put into the thinner quartz tube, and a graphite crucible containing source materials was placed at the tube center. The tube was then sealed, the furnace was heated at a rate of 20 °C/min to 1000 °C, and the temperature was kept constant for over 3.0 h. During the whole synthesis, an Ar flow at a rate of 80 mL/min was kept through the quartz tube and the pressure within the tube was maintained at ∼1 atm. After the furnace cooled to room temperature, the collected black-colored products from the alumina substrate and the inner wall of the thinner tube were characterized using a scanning electron microscope (SEM, Hitachi S-4800) and a transmission electron microscope (TEM; JEM-2100F) equipped with an energy dispersive X-ray spectrometer (EDX) and an electron energy loss spectrometer (EELS). Raman scattering was measured by a laser Raman spectrophotometer (T64000, France) at room temperature.

* To whom correspondence should be addressed. E-mail: hu.junqing@dhu.edu.cn. Fax: 82-2-875-6636. Phone: 86-21-67792947.

10.1021/jp1013434
Published on Web 04/20/2010

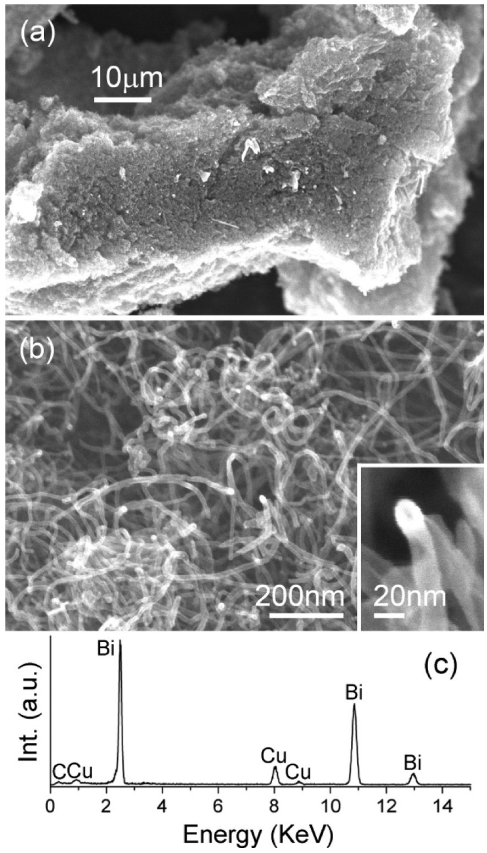

Figure 1. (a) Low-magnification SEM image of as-synthesized product. (b) High-magnification SEM image showing pure and uniform carbon nanotubes. The inset shows a Bi droplet attached to the carbon nanotube tip. (c) The EDX spectrum recorded from the Bi droplet.

The field emission properties were measured using a diode structure in a high vacuum chamber with a base pressure of $\sim 8 \times 10^{-8}$ Torr. A rod-like aluminum probe with a collection area of ~ 1 mm^2 was used as an anode, which was positioned by a linear-motion step controller, and synthesized CNT was used as a cathode. A direct current (dc) voltage, increasing from 100 to 1100 V, was applied to the carbon nanotubes at an anode−sample distance of 200 μm and with an increasing voltage step of 10 V.

Results and Discussion

As-grown product appeared like a black-colored wool on the alumina substrate and the thinner linear quartz tube (downstream); the yield densely and thickly ($\sim$1 mm in thickness) covered a large area of $\sim 20 \times 40$ mm^2, as shown in the low-magnification SEM image in Figure 1a. The high-magnification SEM image, Figure 1b, reveals that as-synthesized product consists of very pure (nearly 100%) and uniformly sized carbon nanotubes with a length of several μm. It is found that some carbon nanotubes are ended or terminated with a hemispherical particle, as shown in the high-resolution SEM inset of Figure 1b. The EDX (with a probe size smaller than $\sim$1 nm) spectrum shown in Figure 1c, which was recorded from the hemispherical particle, confirmed that it was metallic Bi, suggesting the present carbon nanotubes began to grow via a traditional vapor−liquid−solid (VLS) process. Detailed microstructures of the carbon nanotube materials were further investigated using TEM, electron diffraction (ED), and EELS.

TEM examination reveals that as-synthesized CNTs are remarkably uniform and clean; no other carbon allotropes like graphite or amorphous clustered material could be found. Most of the tubes ($\sim$80%) have an outer diameter of $\sim$5−8 nm. Interestingly, individual carbon nanotubes were tipped or terminated with an onion-shaped carbon. A selected area ED pattern taken from many CNTs is shown in the lower left inset in Figure 2a. It exhibits regular reflections, in which the first four ED rings (from the one with the smallest diameter) are in good agreement with the (002), (004), (006), and (008), respectively, atomic plane spacings of the hexagonal graphite (JCPDS card no. 41-1487), indicating that these CNTs have a highly crystalline structure.[14,15] Figure 2b depicts a HRTEM image taken from many tubes; it can be seen that the tube walls are built up of regular, about 5−10, graphitic layers. That is, the tube walls have a thickness of $\sim$2−4 nm. Thus, a large amount of highly graphitic carbon nanotube has been synthesized from a thermal reaction of activated carbon and Bi_2O_3 powders. Keeping in mind that carbon microtubes have been synthesized using a similar technique, we propose that the as-called oxide carbon-thermal reaction may be a universal route toward synthesis of crystalline graphitic carbon micro/nanotubes.[8,9]

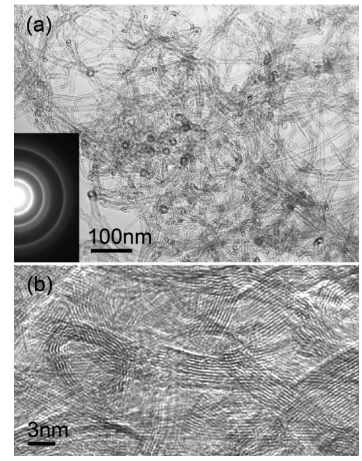

Figure 2. (a) TEM image showing the carbon onion tipped CNTs. The inset shows the ED pattern taken from CNTs in this figure. (b) HRTEM image showing the highly crystalline graphitic structure within the CNTs.

Careful high-resolution TEM imaging of several tens of individual CNTs reveals that the outer diameter and wall thickness of as-synthesized CNTs, as shown in Figure 3a, are $\sim$5−8 and 2−3 nm, respectively. The tube wall is composed of regularly ordered graphitic layers; that is, the tube wall is built up of 5−10 graphitic (002) layers with an interplanar spacing of 0.34 nm within the tube wall. A representative EEL spectrum (recorded using a stationary focused 1 nm electron probe) is shown in the upper right inset in Figure 3a, in which the π^* ($\sim$283.6 eV) and σ^* ($\sim$ 295.6) peaks in the vicinity of the C K-shell ionization edge are clearly displayed. The π^* peak indicates that C is in an sp^2 hybridization state and that the tube is mainly composed of hexagonal graphitic layers, as also suggested by HRTEM. The sharp σ^* peak may indicate the formation of pentagonal defects within graphitic layers.[16] The ED pattern shown in Figure 3c, taken from a domain throughout the tube walls and tube cavity, consists of overlapping diffractions originated from the tube walls and tube cavity and thus exhibits strong (10.0) and (11.0) diffraction rings together with the weak (002) and (20.0) rings. The ED shown in Figure 3d, taken from one side tube wall, exhibits regular reflections, indicating the tube can be regarded as a real "graphitic crystal", which has a "herring-bone" structure.[14,15] In the pattern, a pair of bright arcs peculiar to the (002) reflection is visible along

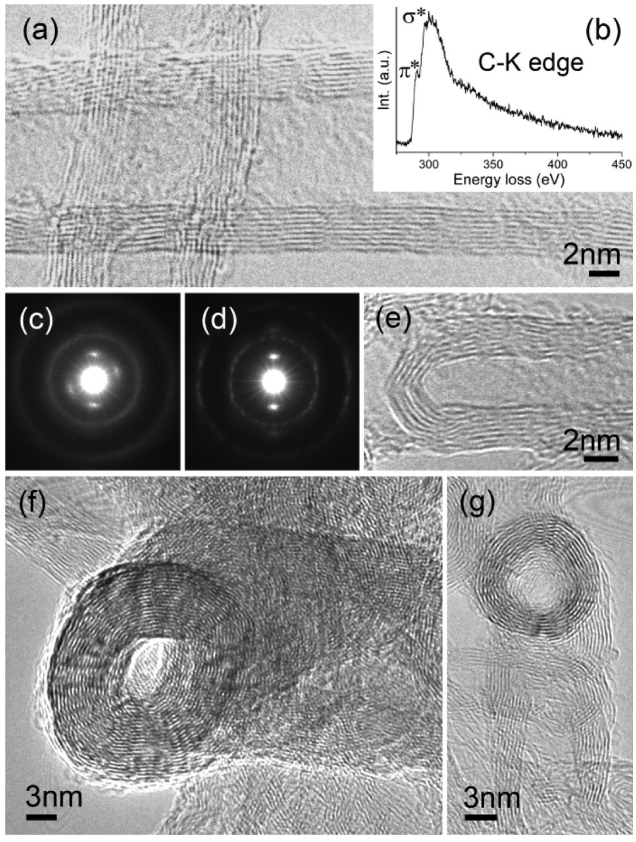

Figure 3. (a) HRTEM image showing the outer diameter and wall thickness of the CNTs. (b) An EEL spectrum recorded from a tube. (c, d) ED patterns taken from a domain throughout the tube walls and tube cavity, and one tube wall, respectively. (e) An HRTEM image of a closed end tube. (f, g) HRTEM images showing different sized carbon tips.

the direction perpendicular to the tube axis, and a pair of (10.0) arcs is seen along the direction parallel to the tube axis. This suggests that the (002) planes near the external edge of the tube are preferentially oriented in parallel to the incident electron beam. Both EELS and ED results suggest that the tube walls consist of cylindrically stacked graphitic (002) planes; thus, it exhibits graphitization analogous to other graphitizing carbons[17] and multiwalled C nanotubes.[1,18] The HRTEM image in Figure 3e reveals that this CNT's end possesses curved lattice fringes, forming a closed tube. Shown in Figure 3f and g are typical HRTEM images of onion-shaped terminated carbon nanotubes. The hollow interior of the tips is surrounded by multiple layers of nested concentric graphite shells that appear as dark lines representing the individual atomic layers. The tips are ~20 nm in diameter (30 layers), and the curved lattice fringes clearly show the proper graphitic interlayer distance of 0.33 nm. Obviously, the slight distortion of spherical shape is due to the defects during the graphitiztion process. It is clear that carbon tips grew on the CNTs' ends, rather than being physically placed on the end surface of the formed CNTs.

Raman scattering was analyzed at room temperature in order to get useful structural information. The representative spectrum, Figure 4, of the sample displays the typical features of multiwalled CNTs.[1,9,19] The G-band centered at ~1572 cm^{-1} is ascribed to the tangential modes of the graphite-like C structure, and the D-band appearing at ~1345 cm^{-1} and the overtones at ~2680 cm^{-1} (2 × D) are usually associated with vibrations of C atoms having dangling bonds due to the in-plane terminations of a disordered graphite.[20]

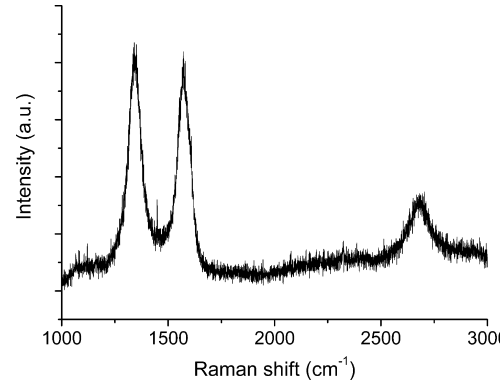

Figure 4. Raman scattering measured at room temperature for these CNTs.

From a chemical reaction point of view, a mixture of Bi_2O_3 and activated carbon underwent the following reactions. Carbonthermal reduction of Bi_2O_3 and CO disproportionation, at proceeding temperature (~1000 °C), which are assumed on the basis of the thermodynamical properties consecutively noted in parentheses below: $Bi_2O_3(s) + 2C(s) \rightarrow 2Bi(l) + CO_2(g)$ (1) ($\Delta G^0_{1273K} = -765.86$ kJ/mol, $\log K^0 = 31.40$), $Bi_2O_3(s) + 2C(s) \rightarrow 2Bi(l) + CO(g)$ (2) ($\Delta G^0_{1273K} = -482.19$ kJ/mol, $\log K^0 = 19.80$), and $2CO(g) \rightarrow CO_2(g) + C(s)$ (3) ($\Delta G^0_{1273K} = -326.13$ kJ/mol, $\log K^0 = 13.38$). As revealed by reactions 1 and 2, the total entropy considerably decreases to form liquid Bi and gaseous CO and CO_2. It is favorable for reactions 1 and 2 with the processing temperature increase. At a temperature as high as 1273 K, Bi_2O_3 reacts with carbon powders to form liquid Bi, CO, and CO_2 due to the negative Gibbs free energy. CO disproportionation (Boudouard reaction) is widely suggested as the mechanism of CNT growth from a CO source[20–26] in which carbon is said to deposit on the liquid droplet surface via the metal catalyzed disproportionation of CO. Here, the metallic catalyst is the as-formed liquid Bi droplet in reaction 1. At the beginning, the Bi droplet is only a few nanometers in diameter. Such a Bi droplet contains a very high percentage of surface atoms, creating a tremendous surface energy per atom. There are two processes to decrease this surface energy. One is the growth process of a CNT. Carbon diffuses into the droplet until a saturation point is reached. Carbon then begins to precipitate and assemble on the surface of the saturated Bi particle, with its edges strongly chemisorbed to the metal Bi, from which a graphene cap or layer can form; for example, an onion-shaped carbon can grow on the surface of this saturated Bi droplet. During the ongoing reaction, more C (clusters) are generated and then accumulate at the boundary of the liquid Bi droplet's surface, resulting in CNTs growing. Finally, as-formed carbon is pushed away from the Bi droplet's surface and lifted upward by the growing CNT, as suggested by the SEM imaging. Also, some small sized Bi droplets undergo agglomeration and are then oxidized to form Bi_2O_3 in an annealing process and decreased temperature process. The source of oxygen that contributed to the formation of Bi_2O_3 may have two origins. The most likely source of oxygen may come from the low content of O_2 (~100 ppm) in the carrier gas of Ar, which can supply a constant oxygen source during the growth of Bi_2O_3. Another likely source is the residual oxygen, as the base pressure within the tube system is maintained at ~1 atm.

To study the performance of the as-synthesized carbon nanotubes' field emitters, voltage was ramped up and $I-V$ data was obtained; the corresponding $I-V$ curve was plotted, as shown in Figure 5a. Here, the threshold field, which was defined

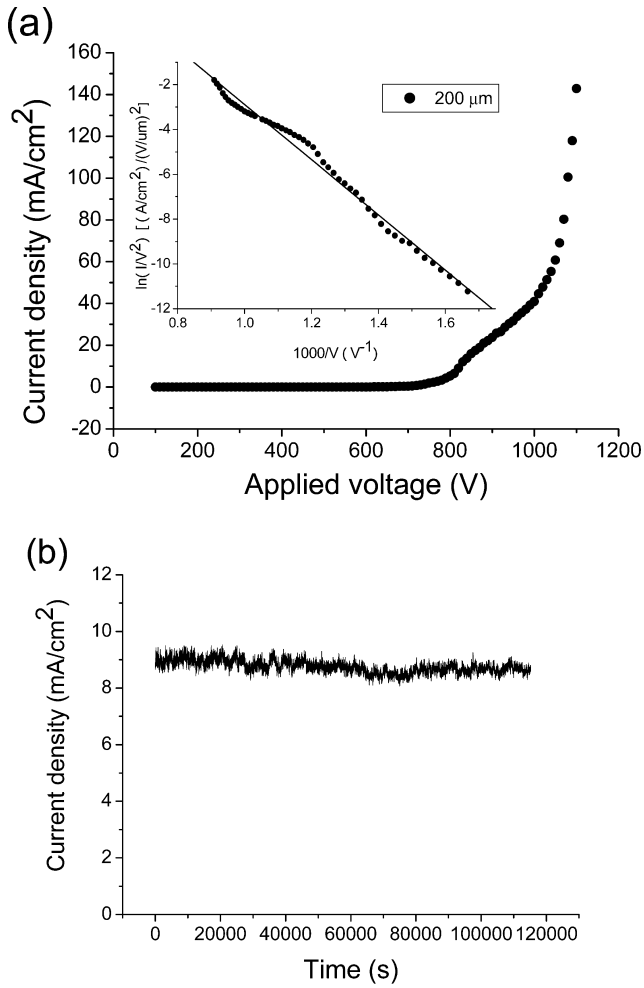

Figure 5. (a) Field-emission date collected from the carbon nanotubes. The inset shows the corresponding F−N plot. (b) The typical fluctuation of the field emitting density with an emission current of ∼9 mA/cm^2 for 32 h.

as the field required to produce an emission current density of 10 mA/cm^2 in dc mode, was calculated to be ∼4.1 V/μm. To our excitement, the synthesized CNTs showed the highest current density of ∼145 mA/cm^2 at a low voltage of 5.5 V/μm. The emission stability of the CNTs was performed with a high emission current density of ∼9 mA/cm^2 and under a constant applied voltage, as shown in Figure 5b. It was found there was no remarkable degradation of the emission current in the testing period of 32 h or more and the degradation rate from the first 1 min to the last 1 min during this testing period was lower than 1%. Thus, it was concluded that the as-synthesized CNTs displayed extremely good emission stability at this high emission current density. To our best knowledge,[27–29] there are few reports that CNTs' emitters have a high current density (of ∼145 mA/cm^2) at such a low corresponding voltage (of 5.5 V/μm); moreover, the reported CNTs' emission performance usually tends to degrade when emitting at a relatively high current density, and thus shows poor emission stability at the high current density.[13,30,31] The present CNTs possessed a high emission current density at a low voltage and a good emission persistence and stability, at a high emission current density. For the CNTs acting as electron emitters, the high emission current density (at a low voltage) and the emission stability (at high current density) are in parallel required for excellent image quality in field emission display fabrication. Therefore, the as-fabricated CNTs will have great potential application in field emission panel displays.

The emission characteristics were frequently analyzed using the Fowler−Nordheim (F−N) theory, which has proven to be useful for describing the field emission from electron emitters from different materials. The emission current density can be represented by the following F−N equation:[32] $I = aV^2 \exp(-(b/V))$, where $b = 0.95B\phi^{3/2}/\beta'$, β' is the local field conversion factor at the emitting surface, a is a constant, $B = 6.87 \times 10^7$, and Φ is the work function of CNTs (∼ 5 eV), which is assumed to be the same as that of graphite. The electric field enhancement factor β can be estimated from the local field (E_{loc}) equation: $E_{loc} = \beta V/d$, where d is the distance between the anode and the cathode. Combining these relationship gives $\beta = 0.95B\phi^{3/2}d/b$, where b is the slope of the F−N plot. The nearly linearity of the plots, as shown in the inset in Figure 5a, indicates that the measured currents are emitted by the field emission mechanism. From the slope of the $\ln(I/V^2)-1/V$ plots, the field enhancement factor β is calculated to be about 5800 for the present CNT sample, which is greatly larger than the best field enhancement factor (<3000) of these nonaligned CNTs in previous literature.[33]

The excellent field emission capability may be related to the perfect graphitization of the CNTs as well as a unique carbon tip on them. The electrons are emitted from both the tubular walls of the CNTs and curved graphitization rings of the carbon onions, in which the latter was regarded as a new emission site. Thus, intensive electrons can be emitted easily even if a small voltage is applied, that is, a high emission current density can be obtained at a low voltage. Additionally, the carrier mobility and conductivity may also play roles in the field emission properties for these special shaped CNTs. The pentagonal defects within graphitic layers of CNTs, as suggested by EEL and Raman spectra, may improve the carrier mobility and conductivity and reduce the current fluctuation. Good emission persistence and stability can be achieved, even at a high emission current density.

Conclusion

In summary, large-scale synthesis of highly graphitic carbon nanotubes (with a diameter of ∼5−8 nm) from a thermal reaction of activated carbon and Bi_2O_3 powders, which was grown *via* a carbon-thermal reduction and Bi catalyzed vapor−liquid−solid process, has been achieved. Individual carbon nanotubes were tipped or terminated with onion-shaped carbon, which has never been observed before in carbon nanotube growth. Keeping in mind that carbon microtubes have also been synthesized using a similar technique, we propose that the as-called oxide carbon-thermal reaction is a universal route toward crystalline graphitic carbon micro/nanotubes. Field emitters made from the present carbon nanotubes exhibit excellent emission properties: they can be operated at a very large current density of ∼145 mA/cm^2 at a low voltage of 5.5 V/μm, and possess a long period (>32 h) of emission stability at a high emission current density of ∼9 mA/cm^2 and under a constant applied voltage. These properties are equally important for high image quality in field emission display fabrication. Hence, these excellent field emission properties suggest that as-fabricated CNTs could be an effective and reliable electron-emitting source.

Acknowledgment. This work was financially supported by the National Natural Science Foundation of China (Grant Nos. 50872020 and 50902021), the Program for New Century Excellent Talents of the University in China, the "Pujiang" Program of Shanghai Education Commission (Grant No. 09PJ51400500), the "Dawn" Program of the Shanghai Education

Commission (Grant No. 08SG32), the Shanghai Leading Academic Discipline Project (Grant No. B603), the "Chen Guang" project (Grant No. 09CG27) supported by the Shanghai Municipal Education Commission and Shanghai Education Development Foundation, the Program for the Specially Appointed Professor by Donghua University (Shanghai, P.R. China), and the Program of Introducing Talents of Discipline to Universities (No. 111-2-04).

References and Notes

(1) Iijima, S. *Nature* **1991**, *354*, 56.
(2) Ren, Z. F.; Huang, Z. P.; Xu, J. W.; Wang, J. H.; Bush, P. *Science* **1998**, *282*, 1105.
(3) Wong, S. S.; Joselevich, E.; Woolley, A. T.; Cheung, C. L.; Lieber, C. M. *Nature* **1998**, *394*, 52.
(4) Tang, Z. K.; Zhang, L. Y.; Wang, N.; Zhang, X. X.; Wen, G. H.; Li, G. D.; Wang, J. N.; Chan, C. T.; Shang, P. *Science* **2001**, *292*, 2462.
(5) Ebbesen, T. W.; Ajayan, P. M. *Nature* **1992**, *358*, 220.
(6) Lee, R. S.; Kim, H. J.; Fischer, J. E.; Thess, A.; Smally, R. E. *Science* **1997**, *288*, 255.
(7) Fan, S. S.; Chapline, M. G.; Franklin, N. R.; Tombler, T. W.; Cassell, A. M.; Dai, H. J. *Science* **1999**, *283*, 512.
(8) Hu, J. Q.; Bando, Y.; Xu, F. F.; Li, Y. B.; Zhan, J. H.; Xu, J. Y.; Golberg, D. *Adv. Mater.* **2004**, *16*, 153.
(9) Hu, J. Q.; Bando, Y.; Zhan, J. H.; Zhi, C. Y.; Xu, F. F.; Golberg, D. *Adv. Mater.* **2006**, *18*, 197.
(10) Choi, W. B.; Chung, D. S.; Kim, H. Y.; Jin, Y. W.; Han, I. T.; Lee, Y. H.; Jung, J. E.; Lee, N. S.; Park, G. S.; Kim, J. M. *Appl. Phys. Lett.* **1999**, *75*, 3129.
(11) Baughman, R. H.; Zakhidov, A. A.; de Heer, W. A. *Science* **2002**, *297*, 787.
(12) Treachy, M. M.; Ebbesen, T. W.; Gibson, J. M. *Nature* **1996**, *381*, 678.
(13) Bonard, J.-M.; Salvetat, J.-P.; Stöckli, T.; de Heer, W. A.; Forró, L.; Châtelain, A. *Appl. Phys. Lett.* **1998**, *73*, 918.
(14) Libera, J.; Gogotsi, Y. *Carbon* **2001**, *39*, 1307.
(15) Gogotsi, Y.; Dimovski, S.; Libera, J. A. *Carbon* **2002**, *40*, 2263.
(16) Hellgren, N.; Johansson, M. P.; Broitman, E.; Hultman, L.; Sundgren, J.-E. *Phys. Rev. B* **1999**, *59*, 5162.
(17) Franklin, R. E. *Proc. R. Soc. London, Ser. A* **1951**, *209*, 196.
(18) Ebbesen, T. W.; Ajayan, P. M. *Nature* **1992**, *358*, 220.
(19) Dresselhaus, M. S.; Eklund, P. C. *Adv. Phys.* **2000**, *49*, 705.
(20) Rao, A. M.; Richter, E.; Bandow, S.; Chase, B.; Eklund, P. C.; Williams, K. A.; Fang, S.; Subbaswamy, K. R.; Menon, M.; Thess, A.; Smalley, R. E.; Dresselhaus, G.; Dresselhaus, M. S. *Science* **1997**, *275*, 187.
(21) Nikolaev, P.; Bronikowski, M. J.; Bradley, R. K.; Rohmund, F.; Colbert, D. T.; Smith, K. A.; Smalley, R. E. *Chem. Phys. Lett.* **1999**, *313*, 91.
(22) Bladh, K.; Falk, L.; Rohmund, F. *Appl. Phys. A* **2000**, *70*, 317.
(23) Nasibulin, A. G.; Moisala, A.; Brown, D. P.; Kauppinen, E. I. *Carbon* **2003**, *41*, 2711.
(24) Moisala, A.; Nasibulin, A. G.; Kauppinen, E. I. *J. Phys.: Condens. Matter* **2003**, *15*, S3011.
(25) Nasibulin, A. G.; Brown, D. P.; Queipo, P.; Gonzalez, D.; Jiang, H.; Kauppinen, E. I. *Chem. Phys. Lett.* **2006**, *417*, 179.
(26) Queipo, P.; Nasibulin, A. G.; Jiang, H.; Gonzalez, D.; Kauppinen, E. I. *Chem. Vap. Deposition* **2006**, *12*, 364.
(27) de Heer, W. A.; Châtelain, A.; Ugarte, D. *Science* **1995**, *270*, 1179.
(28) Zhu, W.; Bower, C.; Zhou, O.; Kochanski, G.; Jin, S. *Appl. Phys. Lett.* **1999**, *75*, 873.
(29) Lee, S. B.; Teo, K. B. K.; Robinson, L. A. W.; Teh, A. S.; Chhowalla, M.; Hasko, D. G.; Amaratunga, G. A. J.; Milne, W. I.; Ahmed, H. *J. Vac. Sci. Technol. B* **2002**, *20*, 2773.
(30) Dean, K. A.; Chalamala, B. R. *Appl. Phys. Lett.* **1999**, *75*, 3017.
(31) Rao, A. M.; Jacques, D.; Haddon, R. C.; Zhu, W.; Bower, C.; Jin, S. *Appl. Phys. Lett.* **2000**, *76*, 3813.
(32) Spindt, C. A.; Brodie, I.; Humphrey, L.; Westerberg, E. R. *J. Appl. Phys.* **1976**, *47*, 5248.
(33) Sveningsson, M.; Morjan, R.-E.; Nerushev, O. A.; Bäckström, Y. S. J.; Campbell, E. E. B.; Rohmund, F. *Appl. Phys. A* **2001**, *73*, 409.

JP1013434